PHOTO-INDUCED PLASTICITY IN AMORPHOUS CHALCOGENIDES: AN OVERVIEW OF MECHANISMS AND APPLICATIONS

M. L. Trunov[*]

Uzhgorod National University, 13, Kapitulna str., Uzhgorod 88000, Ukraine

The athermal increase in the plasticity of glasses has been achieved under the combined action of external stress and illumination. A review has been given on this subject including the change in the plasticity behavior with the sample composition of As_xSe_{1-x} thin films. We suggest that the presence of stress-free phase (close to the mean-field rigidity percolation transition) is the main condition for the giant photo-softening effect observed in thin films of chalcogenide glasses. It is confirmed that the most pronounced negative photo-plastic effect (giant photo-softening) is observed in $As_{20}Se_{80}$ films while change in photo-induced optical constants is the lowest. The results will be discussed within the frame of recent structural models of chalcogenide glasses. Possible applications of the effect of nanoscale photo-induced plasticity of chalcogenide glasses for improvement of the technology of chalcogenide film production and in devices for nanoimprint lithography and opto-mechanical data storage have been considered.

1. Introduction

It is well known from the years '70 of the last century that chalcogenide vitreous semiconductors – i.e., sulfides, selenides, or tellurides, exhibit photoinduced phenomena which are not observed not only in their crystalline counterparts but in the majority of crystalline semiconductors, in general. For example, the interaction of a laser beam with a variety of amorphous chalcogenides (ACh) results in photostimulated changes of their optical, mechanical and chemical properties. The most pronounced effect is observed under band-gap light irradiation with a photon energy $h\nu \geq E_g$ (where E_g is the Tauc optical gap), though the similar changes under sub-band gap light also take place [1]. However, in this paper we consider another type of photo-induced phenomena in ACh – the light-induced plasticity or photo-plastic effect (PhE), which is also typical for crystalline semiconductors. In spite of the fact that the mechanisms of PhE in amorphous and crystalline semiconductors must be fundamentally different, the final results of the effect of light are very close.

The PhE denotes the reversible influence of light on the flow stress and hardness of a material and may be of two types – the positive PhE (if materials become stronger under irradiation) or negative one (if the light-induced softening takes place). Note that for ACh only the second type (photo-softening) of the effect has been observed so far while both light-induced hardening and softening were found for crystals. As regards the PhE in crystalline semiconductors it is assumed that the positive PhE (it dominates in II-VI group substances) occurs in the materials where charge carriers generated by irradiation modify the charging of dislocations or charge state of electrically active point defect, and the negative PhE (it dominates in III-V group substances) is explained in terms of non-radiative recombination at the energy of traps and the resulting local heating decreases

---

[*] Corresponding author: stm@tn.uz.ua

the barriers of dislocation movement. Since amorphous semiconductors are a very unusual disordered structure in which the dislocations are absent and the motion of point defects cannot occur in the same way as in crystals, quite another mechanism takes responsibility for the PhE in these materials. Possible mechanisms of the PhE in ACh and some practical applications are the subjects of this paper.

First of all we have briefly reviewed the history of the discovery of athermal plastic changes in the structure of materials which are governed by light, and then the synopsis of structural models has been given. Some of these models have been chosen to examine the experiment and finally, some possible applications of the PhE have been discussed.

The light-induced plasticity of the substances has been studied intensively during the last few decades. The main tool of PhE investigations is the uniaxial deformation experiment and surface hardness measurements. Both macroscopic indentation and nanoindentation in bulk and film samples have been investigated in detail. We have tried to summarize all these investigations in Table 1 [2-15].

After first report made by Vonwiller at the beginning of 20th century [2] subsequent experiments performed by various scientific group show that the PhE exists in a broad variety of materials both crystalline and non-crystalline semiconductors, organic polymers (polycarbonate) and even ice single crystal (see Table 1). Note, that numerous names were used for the effect detected in amorphous semiconductors though the essence of the phenomena observed by the investigators was the same. So, after Deryagin's report [5] about decrease of surface microhardness in film samples caused by light and Nemilov's observation of light-induced reduction of viscosity in bulk samples near T_g [6] , the negative PhE was found for As-S(Se) films under band-gap light irradiation [7,8]. The macroscopic model of this phenomenon was based on suggestions of the reduction of viscosity of films to 10^{12}-10^{13} Poise which is achieved by an athermal way and is comparable to that obtained above the glass-transition temperature T_g. This suggestion was confirmed later by direct experiments [8].

The following observations of the PhE under a low temperature in the amorphous selenium (optical melting [13]), the fluidity [10], one of the facets of the PhE under sub-gap excitation, discovered for As_2S_3 fibers and flakes, as well as the presence of the PhE temperature hindering [9,10]) pointed out to the universal nature and unique mechanism of the phenomena observed. However this mechanism is speculative and not clear so far.

Several models have been proposed to describe ACh plasticity induced by light irradiation:
1. H.Fritzsche's model [17]. This model has found wide application for ACh and used the Street idea about non-radiative recombination of photo-excited electron-hole pairs through an intermediate transient exciton formation with the changes in the coordination number and the charge state of pnictide and chalcogenide atoms. The exciton recombination led to a local rearrangement of bonds and new configuration appears which is different from initial configuration. The cumulative effect of local configuration changes involving essentially all atoms produces such a macroscopic phenomenon as the fluidity, if the external stresses were applied to the sample.
2. J. Li's and D.A. Drabold's model [18]. For development of this model the first-principle molecular dynamics simulation was used. From this simulation and under the consideration of defect chemistry of ACh it was shown that defect pairs (the so-called HOMO and LUMO groups) associated with band tail states become involved in the rearrangement in the covalent network. Under irradiation the plasticity arises due to the diffusion motion which is observed for short times.
3. K. Tanaka's model [19]. The localized sites which appear due to electron and holes excited by light act as "knots" of the segmental structure and the plasticity of the material increases. If the material is subjected to stresses such atomic changes as the macroscopic fluidity will appear.
4. H. Oyanagi et al.'s model [13]. In this model the photo-induced non-thermal melting in ACh (a-Se) is interpreted as the result of pairing of excited lone pair electrons which induce neutral three –fold coordinate pairs. As a result, the formation and breaking of interchain bonds appear which reduce the rigidity of the network
5. K. Shimakawa's model [20]. The "slip and repulsion model" that has been proposed first of all accounts for the photodarkening and photoexpansion in ACh. The model was based on the idea that layer-like clusters that exist in ACh and are located in the illumination region become negatively

charged due to different mobility of charge carriers. As a result, the electrostatic repulsion forces arise between adjacent layers. Regarding photoplasticity it is concluded that the mutual glide motion of the layers after applying the external stress will be achieved more easily in such a case.

6. S. Yannopoulos' model [21]. From Raman-scattering studies on sub-gap excitations the probable model of photo-induced plasticity has been given, based on effective unfolding of As_4S_4 cage-like molecules realized by the combined action of light and stress. The term "photoductility" is proposed as the name of the effect. It's very interesting that the concentration dependence of the effect is considered in this model only.

On the one hand Yannopoulos' model confirms that specific cage-molecules $As_4S_4(Se_4)$ and/or $As_4S_3(Se_3)$- types are responsible for the PhE. It is very essential that the same structural units are considered for the explanation of the well-known photo-induced changes of the optical constants in ACh, both in bulk and film forms. The concentration of such structural units reaches the maximum in composition, which is close to stoichiometric one, i.e. to $As_{40}S_{60}$ and $As_{40}Se_{60}$, as well as in those in which As-As bonds are dominant ($As_{44}S_{66}$ and $As_{50}Se_{50}$). In this case a strong correlation will be observed between the light-induced plasticity and the photo-induced change in optical constants. The maximum of these changes must be very close to the stoichiometric composition.

Table 1. Photoplasticity in solids: evolution of observations from 1919 to 2004.

Author(s)	Name of the effect	Materials	Light source	Method	Comments on the essential features of the observed effect
O. U. Vonwiller (1919) [2]	No name	a-Se and c-Se (bulk)	Unknown	No details	Observation of the effect of light onto the plasticity of solids
G. C. Kuczynski, R. F. Hochman (1957) [3]	Photomechanical effect	n-type Ge, InSb, InAs and p-type Si (bulk)	Mercury lamp	Microhardness measurements	Decrease in micro hardness in crystalline semiconductors
Yu. A. Osipyan, I. B. Savchenko (1968) [4]	Photoplastic effect	crystalline CdS (bulk)	Electrical lamp with a filter	Compressive testing	The effect of light on stress flow and the strength limit in crystals
B. V. Deryagin, Yu. A. Toporov, K. I. Merzhanov et al. (1974) [5]	Photomechanical effect	a-Se, a-As_2S_3 (films)	Electrical lamp with a filter	Microhardness measurements	Decrease in micro hardness in amorphous semiconductors
S. V. Nemilov, D. K. Tagantsev (1981) [6]	Photoviscosity effect	a-As_2S_3, a-As_2Se_3 (bulk)	Bandgap illumination (laser)	Viscosity measurements near T_g	Decrease in viscosity under illumination with one order magnitude from dark one
M. L. Trunov, A. G. Anchugin (1992) [7-9]	Photoplastic effect	a-As_2S_3, a-As_2Se_3 (film)	Bandgap illumination (laser)	Internal stress relaxation and microhardness measurements	Athermal decrease in viscosity to 10^{12}-10^{13} poise under bandgap illumination. The temperature hindering of the effect
H. Hisakuni, K. Tanaka (1995) [10]	Photofluidity	a-As_2S_3 (fiber/flake)	Subbandgap illumination (laser)	Tensile testing	Athermal decrease in viscosity to $5 \cdot 10^{12}$ P under subbandgap irradiation
N. Khusnatdinov, V. F. Petrenko (1994) [11]	Photoplastic effect	ice single crystals	Ultraviolet illumination with xenon lamp	Compressive testing	Observation of hardening in an ice crystal under illumination

Author(s)	Name of the effect	Materials	Light source	Method	Comments on the essential features of the observed effect
P. Krecmer, A. M. Moulin, R. J. Stefenson et al. (1997) [12]	Opto-mechanical effect*	a-As$_{50}$Se$_{50}$ (film)	Bandgap illumination (laser)	Internal stress relaxation measurements	Observation that stress depends upon polarization of the incident light
H. Oyanagi, A. Kolobov, K. Tanaka (2000) [13]	Optical melting	a-Se, a-As$_2$Se$_3$ (film)	Xenon lamp	X-ray absorption spectroscopy	Reports on melting phenomenon under light illumination at low temperature, 30K
R. Bajpai, S. Sharma et al. (2003) [14,15]	Photoplastic effect	Polycarbonate	Mercury lamp	Microhardness measurements	First report of the photoplastic effect in organic polymers
M. L. Trunov, V. S. Bilanich (2004) [16]	Polarization-dependent photoplastic effect*	a-As$_{50}$Se$_{50}$ (film)	Bandgap illumination (laser)	Internal stress relaxation and microhardness measurements	Observation that stress relaxation and microhardness of the films depend upon the polarization of the incident light

On the other hand, the giant photo - softening has been detected recently by Brillouin scattering in Ge$_x$ Se$_{1-x}$ glasses with x close to mean- field rigidity percolation transition and it is achieved for Ge$_{19}$ Se$_{81}$ glasses [22]. It looks as a general rule for observation of the giant photomechanical response in glasses and the same approach may be applied for ACh of another composition in which the percolation theory is developed [23,24].

In this paper the last two ideas have been examined and checked by using the As-Se glass as a model system.

2. Experimental

The experiments were performed on 2-μm thick films prepared by thermal evaporation of As$_x$Se$_{1-x}$ glasses (for x = 0, 10, 20, 30, 40 and 50) from quasi-closed effusion cells and deposition at a rate of 2-5 nm/s onto unheated glass substrates. We choose this system for two reasons: (i) thin films of all compositions from amorphous Se to binary As$_{50}$Se$_{50}$ alloys correspond to the starting glass well [25]; (ii) the deviations in the illumination energy E$_{ill}$ to bandgap energy E$_g$ ratio are much smaller than in the case of As-S and Ge-Se glasses [26]. The samples were exposed to radiation of a laser operating at a wavelength of 630 nm. The radiation power density at the sample surface under nanoindentation tests did not exceed 30 mW/cm^2.

Before the experiments the films were kept in dark at room temperature for about 3 months. The films were irradiated from the bottom of samples through transparent substrates∗. The mechanical properties of the deposited films were studied by the method of repeated indentation which is described earlier in detail [27]. Five samples prepared in one deposition cycle were tested. Mainly nanoindentation tests were carried out and preliminary results were given in [28-30]. The diameter of samples was 15 mm and allowed us to carry out multiple measurements to obtain reliable and reproducible results.

---

* Vectoral effect. It is not considered in this paper.

∗ As the light penetration depends on the absorption coefficient which was defined by the film composition we must use the samples with different thickness for every composition to reduce the possible influence of the difference in the layer absorption onto the results of nanoindentation. To avoid this effect the irradiation of the films must be conducted through an indenter. However, the typical construction of a nanohardness tester does not allow it.

Nanoindentation measurements were performed using a depth-sensing nanohardness tester (model Nanoindenter II, MTS Systems) with a Berkovich diamond pyramid as an indenter. The details of instruments and methods are given in [31]. For the experiment we used the step loading (see Fig.1, curve 1): the load schedules comprised first a load ramp to the peak load of 2 mN with a rate of 0.7 mN/s, followed by holding at the peak load for a duration of 60 s, then unloading with the same rate and followed by holding at the zero load for a duration of 60 s. The nanohardness (H) and Young's modulus (E) were calculated from the load–displacement curves according to the Oliver and Pharr procedure [32] with a typical error of ± 0.1 GPa and ± 1 GPa, respectively. Each set of nanoindentation measurements consists of 5 tests for each sample: two tests in darkness (before and after irradiation, respectively) and three one during irradiation.

3. Results and discussion

Fig. 1 (curves 2-4) shows an example of nanoindentation obtained in the series of experiments (at a load of P = 2 mN) with as-deposited $As_{30}Se_{70}$ film. The measurements were performed in the dark (2), during the first exposure, which is started with loading simultaneously (3), and during prolonged irradiation (4). For the films of other composition the obtained dependences were the same and differ only quantitatively.

Similarly with the studies of retarded elasticity in glasses by the deformation relaxation method [33] the total depth of indenter penetration under unloading may be signed as: $h_t = h_e + h_r + h_p$, where h_e is an elastic component, h_r and h_p are relaxation and plastic ones, respectively (see example for curve 3 in Fig.1.).

As it can be seen from the experimental data, the depth of indenter penetration only very slightly depends on holding the indenter under constant load in the dark and after irradiation and the depth recovery is defined by elastic components h_e during fast unloading (Fig. 3, curve 2). The contribution of a relaxation component h_r in the process of depth recovery is very small.

For the measurements in the course of irradiation the pattern is significantly different, whereby the indenter penetration nonlinearly varies with time and the interrelationships between the magnitude of h_e, h_r, h_p change essentially. In the initial and prolonged stage the indenter penetration depth increases sharply (Fig. 1, curve 3 and 4, respectively) and after unloading we can observe the depth recovering due to the increase in the contribution of h_r component.
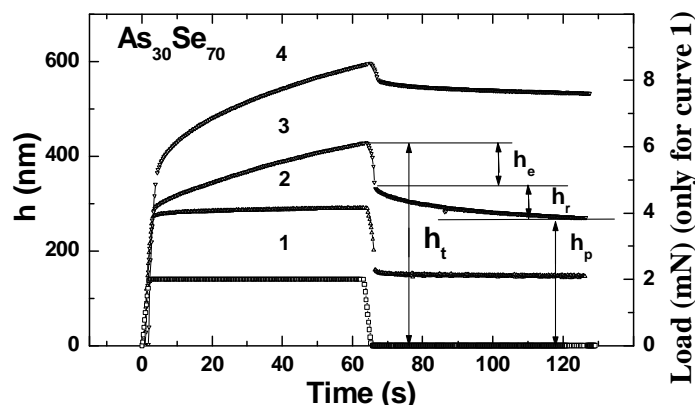

Fig. 1. Depth-time dependences of an indentor penetration at nanoindentation tests of $As_{30}Se_{70}$ films: in the dark (2) and at different stages of irradiation (3 and 4 correspond to the second and third test cycles), 1 – schedule of the tests.

The results obtained reflect the dynamics of photo-induced redistribution of components h_e, h_r, h_p. This dynamics as well as changes in nanohardness and Young's modulus under light irradiation are shown in Fig. 2 for $As_{30}Se_{70}$ film. It is seen that dynamic changes are observed not

only for components h_p (1), h_e (2), h_r (3) but for nanohardness (4) and Young's modulus E (5) either. Thus, at the initial stage of irradiation a step increase in a plastic component and Young's modulus∗ and, simultaneously, the decrease in an elastic component and nanohardness are observed (Fig. 2, curves 1, 5 and 2, 4, respectively). In particular, a plastic component at the initial moment of irradiation for $As_{20}Se_{80}$ rises for 30%, and nanohardness decreases by a factor of 2.

According to the data obtained in all test cycles one can get the concentrational dependence of PhE parameters in As_xSe_{1-x} films. It is known [34] that the energy absorbed by a sample per one cycle of loading at nanoindentation is defined by the loop square of "loading-unloading" cycle on "force-displacement" diagrams. The main parameter which defines the magnitude of this energy is the plastic component, h_p. Taking into account that under irradiation the change in a relaxation component weakly depends on the composition (Fig. 2, curve 3), the dynamic changes of absorbed energy ΔW at nanoindentation during irradiation in films in the first approximation are defined by the redistribution of components h_p and h_e (as $h_r < h_e < h_p$) and, consequently, will be proportional to square ΔS under curve $h_p(t)$ (it is cross-hatched in Fig.2). The photomechanical susceptibility factor of a material defining its sensitivity to irradiation and presenting the degree of structural changes during exposure may be used as one of the PhE parameters. This magnitude is equal to the rate of change in a plastic component dh_p/dt and may be defined from two test cycles – dark and first cycle at irradiation of the sample.
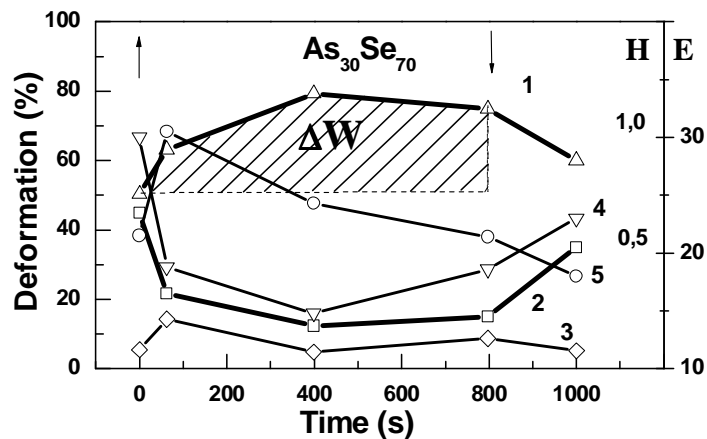

Fig. 2. Dynamics of photomechanical response for $As_{30}Se_{70}$ film: 1-3 – components of total deformation of films at nanoindentation (plastic h_p (1), elastic h_e (2) and viscous h_e (3)), curves 4 and 5 – changes in nanohardness (H) and Young's modulus (E) of the film, respectively. The cross-hatched area is proportional to dynamic changes of energy ΔW, absorbed by the sample in nanoindentation cycles under irradiation. The arrows show switching the light on (↑) and off (↓).

In Fig. 3 the concentrational dependences of above-mentioned values $\Delta W(x)$ in relative units (curve 1) and dh_p/dt (x) (curve 2) are given. From the results obtained it follows that in the region of concentrations of Se atoms close to 80 at. % for both parameters the maximum is observed showing giant changes in the mechanical flexibility of the material under exposure. Simultaneously, for films of this composition the absorbed energy considerably increases during nanoindentation. For example, in comparison with amorphous selenium and $As_{40}Se_{60}$ in $As_{20}Se_{80}$ films the rate of plastic deformation increases by a factor of 5. Similarly, the maximum of absorbed energy in nanoindentation cycle is also observed in $As_{20}Se_{80}$ films. At the same time the photo-induced optical changes for $As_{20}Se_{80}$ films are the lowest compared to other compositions of As-Se system (Fig. 3,

---

∗ It should be noted that the Young's modulus of the film at the initial stage of irradiation increases, whereas nanohardness drops more than by half, although these characteristics usually exhibit direct correlation. Discussion of this fact is outside the scope of this paper, however such behavior was observed in all the samples tested. At the same time the Poisson ratio may also change under irradiation, but we consider it as a constant value close to $\nu = 0.3$ in these measurements.

curve 3). The data obtained point to the dependence of PhE intensity in the given materials on their structure and availability of certain structural elements.

It is known that the concentrational dependence of physical properties of glasses is defined by changing the ratio of structural units, as well as by the availability of the defect subsystem [35]. These structural units define the fundamental properties of a glass, in particular the availability of the number of relaxation transitions from one deformation state into another – the total relaxation spectrum. Each process is defined by unfreezing the mobility of certain kinetic units and accompanied by corresponding effects on temperature and frequency dependences of physical parameters of glasses.
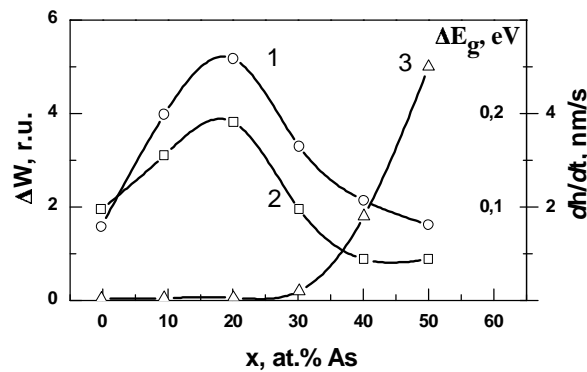
Fig. 3. Concentrational dependences of increment of absorbed energy ΔW (1) and photomechanical susceptibility dh_P/dt (2) at PhE. Curve 3 – photoinduced changes in the forbidden gap for As_xSe_{100-x} films (after [36]).
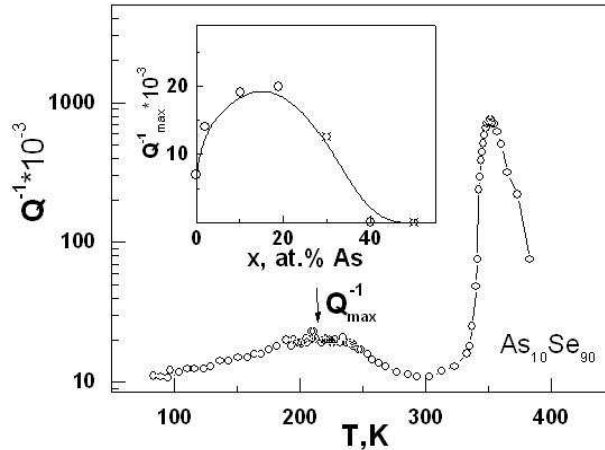

Fig. 4. Temperature dependence of internal friction of $As_{10}Se_{90}$ bulk glasses and concentrational dependence of β – relaxation in As_xSe_{100-x} glasses (inset) [after (37)].

To study the mobility of structural units and defect subsystem and to establish possible correlation of structural relaxation and PhE in As_xSe_{100-x} system we have used the data obtained while studying glasses of As-Se system within 77 K— T_g by the method of internal friction under quasistatic loads at frequencies of $10^{-3} \div 10^{-1}$ Hz [37]. The details of experiments and method of defining temperature-frequency dependences on internal friction Q^{-1} and shear modulus G are described in [38].

In Fig. 4 the dependences Q^{-1} (T) for $As_{10}Se_{90}$ bulk glasses are given. From Fig. 4 it is seen that a wide internal friction maximum with amplitude $Q^{-1}_m = 20 \times 10^{-3}$ is observed within

T_m ~200 K – 220 K which is accompanied by a sharp decrease in shear modulus* $\dfrac{G_0 - G_\infty}{G_\infty} = 0.1$

(10%) (where G_0 and G_∞ are the non-relaxed and relaxed values of shear modulus, respectively). With increasing the deformation frequency the temperature of this maximum T_M rises and the temperature at which G decreases shifts upwards. This indicates the relaxation character of the process which defines the appearance of this maximum.

The maximum losses of internal friction and shear modulus defect value are the largest in $As_{20}Se_{80}$ glass (Fig. 4, inset). In $As_{40}Se_{60}$ и $As_{50}Se_{50}$ glasses the indicated internal friction maximum and shear modulus defect are absent. At the same time in the glassy selenium such maximum is revealed, though it is more weakly pronounced ($Q^{-1}_m = 7 \times 10^{-3}$, see Fig. 4, inset). Taking into account this and the fact that at equal deformation frequency the temperature T_M of internal friction maximum of As_xSe_{100-x} glasses does not depend on the concentration, one can suppose that chalcogen atoms are responsible for above-mentioned maximum.

It is known that the amorphous selenium structure is formed by Se_n chains and rings [39]. It is evident that while adding small amounts of As atoms (the coordination number z = 3) into Se (z = 2) the As-Se bonds are mainly formed by breaking Se_n rings and chains. The number of atoms with broken bonds at the ends of Se_n chains rises. On average, adding one arsenic atom results in one broken bond of selenium (end atoms of chains and rings) in the structure of As_xSe_{100-x} glass. In the region of small concentrations of arsenic atoms As_xSe_{100-x} glasses have an one-dimensional linear-chain structure similar to Se_n one. With further increasing the concentration of arsenic alongside with the process of breaking bonds the formation of chemical As-Se bonds becomes essential due to saturation of broken Se bonds whose concentration in As_xSe_{100-x} glasses at x ≈ 20 is already large, while the length of Se_n chains considerably decreases. In the region of concentrations of selenium atoms x ~ 15-20 % the processes of breaking chains and saturating broken bonds by arsenic atoms have an equal intensity and the concentration of selenium atoms with broken bonds is maximal. Because of this the maximum is observed on the dependence curve Q^{-1}_m (x) in the region of 15-20 at. % of As concentration. Further increase in As concentration results in the decrease of the concentration of Se atoms with broken bonds and as a result the maximum height of internal friction decreases much, and the absolute magnitude of the shear modulus increases.

From Fig. 4 it is seen that in the region of glass transition temperature a strong increase of mechanical losses and decrease in shear modulus are observed. Their temperature position is frequency-dependent: they shift to higher - temperature region with increasing the frequency. Similarly to polymers [40] and oxide glasses [41] one can state that the increase in mechanical flexibility and internal friction of As_xSe_{100-x} glasses in T_g region is defined by the main relaxation process – the so-called α-relaxation, connected with complete unfreezing of segmental mobility of the structure. According to the classification of relaxation transitions in polymers and glasses [40,41], the first relaxation process observed at temperatures lower than α-relaxation (i.e. T < T_g) is called β - relaxation. Thus, it can be concluded that a low-temperature (200-250 K) process of mechanical relaxation in As_xSe_{100-x} glasses is β - process. Taking into account the concentrational changes of its intensity (Fig. 4, inset) one can suppose that it is connected with local relaxation of the structure in the vicinity of selenium atoms with dangling bonds.

Proceeding from the concentrational dependences of PhE parameters in As_xSe_{100-x} films (see Fig. 3) and intensity of β-relaxation (Fig. 4, inset) in the bulk glasses of similar composition one can suppose that between these phenomena a strong correlation and interrelationship of β- relaxation and giant magnitude of photoplastic effect should exist.

4. General remarks

The ability to manipulate the mechanical properties of ACh by photo-modification makes the field fascinating. Note that earlier the giant photoexpansion, in which the photoplasticity plays a key

---

* it is not shown on the Fig. 4.

role, was employed for the shape modification of the ACh surface, in particularly to produce optical microlenses [42]. That is why a particular focus of these concluding remarks is the application of the PhE. One possible way of employing the PhE is to improve the technology of ACh film production and a second one is its using in nanoimprint technique for various purposes.
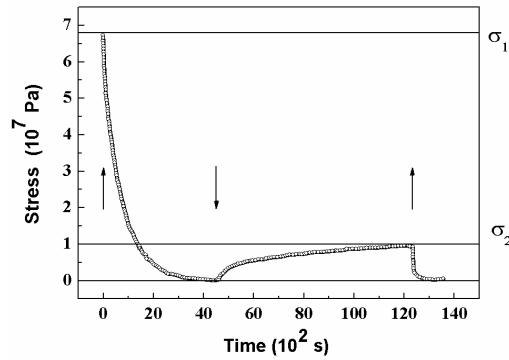

Fig. 5. Mean stress in a 3-μm-thick annealed As_2Se_3 films versus the exposure time: σ_1 − stress after thermal treatment and σ_2 - stress after irradiation. Arrows indicated the moments of light switching on ($\uparrow$) and off ($\downarrow$).

One application of the PhE in technology is to create the stress-free film specimens, because in the process of irradiation the film becomes visco-elastic and the internal stress relaxes to zero (Fig. 5). This can be accomplished by different ways: (i) by irradiating a substrate under a laser during the process of film deposition; (ii) by irradiating the film after the process of deposition being finished; (iii) by choosing the desirable stress on level and sign (they are useful tools if the multilayer samples are produced) through irradiation of the films obtained at different substrate temperature.

The changes in adhesion strength under irradiation take place simultaneously with stress relaxation in thin films. Fig. 6 shows the indentation - time dependence of the imprints obtained during the microindentation test. As we can see the detachment of the annealed film takes place just upon the short contact of the indenter with the film (Fig. 6, row I). With increasing the indentation time (τ_{ind}) the radius and the height of the circle crack grow up. The row II in Fig. 6 shows the changes in these values, when a film is irradiated from the side of the substrate by He-Ne laser in the process of microindentation. It is seen that in this case the film detachment takes place much later (at τ_{ind} = 7-8 min), with the crack height tendency to decrease (at τ_{ind} = 10 min by a factor of 2). For the films preliminarily irradiated during the time equal to τ_{ind} (Fig. 6, row III) the process of film detachment begins at higher value of τ_{ind} ~ 25 min and the crack radius and height are lower.

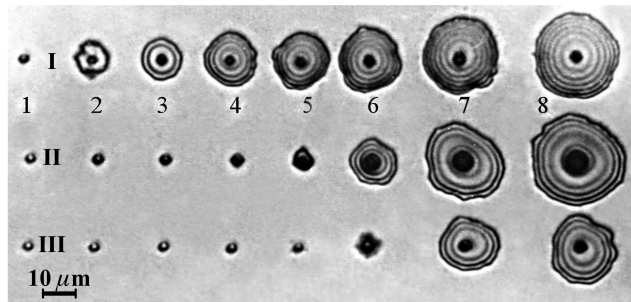Fig. 6. The imprints after sequential microindentations in a 3-μm - thick annealed $As_{40}Se_{60}$ film at a load of P =50 mN in the dark (row I), under irradiation (row II) and after irradiation (row III). The duration of every next load-unload cycle in rows I-III increases with the number, amounting to 10 s (1), 30s (2), 1 min (3), 3 min (4), 5 min (5), 10 min (6), 30 min (7), and 60 min (8). A Vickers indenter was used in all the tests.
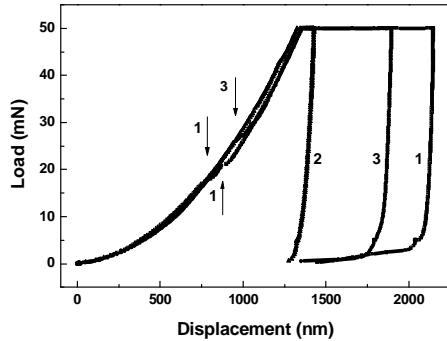
Fig. 7. Load-displacement curves during nanoindentation in a 2-μm - thick annealed $As_{40}Se_{60}$ film. Arrows indicate the moments in which delamination occurs.
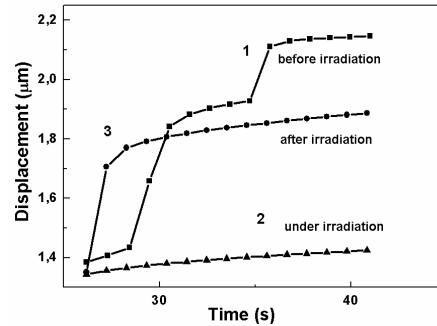
Fig. 8. Creep displacements in a 2-μm - thick annealed $As_{40}Se_{60}$ film tested by nanoindentation which were obtained from curves on Fig. 7 (see the text for explanation).

We also confirmed the improvement in adhesion strength by using nanoindentation test. Fig. 7 shows the load-displacement curves during nanoindentation of 2 μm - thick as-deposited $As_{40}Se_{60}$ film before (1), under (2) and after laser irradiation (3). The change in critical load in which detachment occurs is clearly seen from comparison of curves 1 and 3. It is interesting that the mechanism of failure of a thin film is quite different for a non-irradiated sample and irradiated one. It is reflected by curves 1 and 3 in Fig. 8 in which the displacement-time dependences present the holding segments of the tests corresponding to appropriate curves in Fig. 7. This difference is not clear, and now it is under investigation. Note that under the combined of laser exposure and nanoindentation the film detachment was not observed (Fig. 7, curve 2) even during holding under the maximal load of the test (50 mN) (Fig. 8, curve 2).

A second possible application of the PhE can be the fields of data storage technology and nanoimprint lithography. It is now practicable to use AFM technology to modify the surfaces of materials on the nanoscale [43] and the PhE can be employed both with the possibility of using an AFM tip for writing and readback of topographic features of surfaces for the purpose of data storage. We have proposed the device in which the write mechanism is photo-mechanical by origin (Fig. 9). To write a bit (illustrated in Fig. 9) an AFM-type tip is pressed against a thin film of ACh as the storage medium simultaneously with a laser pulse to produce a nanoscale indentation due to film photoplasticity. To read a bit, the tip is scanned across the indentation and its position which varies depending on whether a pit present or not, is sensed by a position-sensitive detector. This device is similar to those which employ the heating technique for thermo-mechanical data storage [44] and in principle can be modified like IBM Millipede system in which a two-dimensional array of AFM-type tips is used to write and read data in a polymer medium [43].
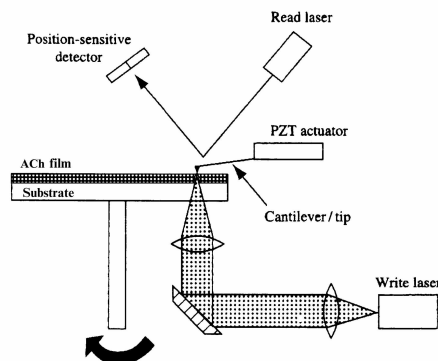
Fig. 9. Setup of the photo-mechanical scanning probe storage system using ACh film as recording media.

On the other hand the PhE can be used in nanoimprint lithography in which a laser-assisted photo-mechanical imprinting of ACh film is capable of producing various nanostructures transferring them from the mold. A nanopattering technique in this case may be similar to traditional one [45]. The main advantage of photo-mechanical imprinting comparatively to photo-thermal one is that it avoids the thermal process, because heating resist is often slow and creates the thermal expansion difference between the mold and substrate that could result in misalignment.

5. Conclusions

Thus, it has been established for the first time that in $As_{20}Se_{80}$ films a giant PhE is observed as a result of which an essential redistribution of deformation components with a sharp rise of plastic component contribution takes place. The absence of correlation between the magnitude of photo-induced optical changes and PhE amplitude in As-Se films has been found.

Based on a good correlation of PhE parameters and internal friction data it is shown that the giant PhE is connected with the maximal concentration of chalcogen atoms with broken bonds in As_xSe_{100-x} films at $x = 20$ at.% and defined by intensive structural rearrangements in such regions of local disordering of the structure. Possible applications of the PhE for improvement of the technology of ACh film production and scanning-probe based storage were considered.

Acknowledgements

References

[1] K. Tanaka, Curr. Opin. Solid State Mater. Sci. **1,** 567 (1996).

[2] O. U. Vonwiller, Nature **104**, 347 (1919).

[3] G. C. Kuczynski, R. F. Hochman, Phys. Rev.B **108**, 946 (1957).

[4] Yu. A. Osipyan, I. B. Savchenko, Pis'ma v ZhETF (Sov. JETP Letters) **7**, 130 (1968).

[5] B. V. Deryagin, Yu. P. Toporov, K.I. Merzhanov, N. M Gal'vidis, I. N. Aleinikova, L. N. Burta-Gaponovich, Fizika Tverdogo Tela **16**, 1780 (1974) [Sov. Phys. Solid State **16**, 1155 (1974)].

[6] D. K. Tagantsev, S. V. Nemilov, Fizika I Khimia Stekla **7**, 195 (1981) [Sov. J. Glass. Phys. Chem. **89**, 220 (1990)].

[7] M. L. Trunov, A. G. Anchugin, Pis'ma Zh. Tekh. Fiz. **18**, 37 (1992) [Sov. Tech. Phys. Lett. **18**, 14 (1992).

[8] M. L. Trunov, A. G. Anchugin, Pis'ma Zh. Tekh. Fiz. **18**, 78(1992) [Sov. Tech. Phys. Lett. **18**, 158 (1992)]; see also a review: M. L. Trunov, J. Non-Cryst. Solids **192/193**, 431 (1995).

[9] M. L. Trunov, A. G. Anchugin, Proc. 5-th Ukr. Conf. On Physics and Technology of Complex Semicond. Thin Films, Uzhgorod, Ukraine, 1992, p.38.

[10] H. Hisakuni, K. Tanaka, Science **270**, 974 (1995).

[11] N. N Khusnatdinov, V.F. Petrenko, Phys. Rev. Lett. **72**, 3363 (1994).

[12] P. Krecmer, A. M. Moulin, R. J. Stephenson, T. Rayment, M. E. Wellard, S. R. Elliott, Science **277**, 1799 (1997).

[13] H. Oyanagi, A. Kolobov, K. Tanaka, Phase Transition **00**, 1 (2000).

[14] R.Bajpai, S. Sharma, V. K. Vastal, B. P. Chandra, Bull. Mater. Sci. **26**, 537 (2003).

[15] S. Sharma, R. Bajpai, B. P. Chandra, J. Appl. Polym. Sci. **90**, 2703 (2003).

[16] M. L. Trunov, V. S. Bilanich, J. Optoelectron. Adv. Mater. **6**, 157 (2004).

[17] H. Fritzsche, Sol. State Commun. **99**, 153 (1996).

[18] J. Li, D. A. Drabold, Phys. Rev. Lett. **85**, 2785 (2000).

[19] K. Tanaka, C. R. Chimie **5**, 805 (2002).

[20] K. Shimakawa, N. Yoshida, A. Ganjoo, Y. Kuzukawa, J. Singh, Phil. Mag. Lett. **77**, 153 (1998).

[21] S. N. Yannopoulos, Phys. Rev. B **68**, 064206 (2003).

[22] J. Gump, I. Finkler, H. Xia, R. Sooryakumar, W.J. Bresser, P. Boolchand, Phys. Rev. Lett. **92**, 245501 (2004).

[23] D. G. Georgiev, P. Boolchand, M. Micuolaut, Phys. Rev. B **62**, R9228 (2000).

[24] S. Mamedov, D.G. Georgiev, Tao Qu, P. Boolchand, J. Phys.: Condens. Matter. **15**, S2397 (2003).

[25] V. I. Mikla, A. A. Baganich, A. P. Sokolov, A. P. Shebanin, Phys. Stat. Sol (b) **175**, 281 (1993).

[26] R. A. Street, R. J. Nemanich, G. A. N. Conell, Phys. Rev. B **18**, 6915 (1978).

[27] M. L. Trunov, Pis'ma Zh. Tekh. Fiz. **30**, 49 (2004) [Sov. Tech. Phys. Lett. **30**, 865 (2004)].

[28] M. L. Trunov, S. N. Dub, R.S. Shmegera, J. Optoelectr. Adv. Mater. **7**, 619 (2005).

[29] M. L. Trunov, S. N. Dub, R.S. Shmegera, Pis'ma Zh. Tekh. Fiz. **31**, 31 (2005) [Sov. Tech. Phys. Lett. **31**, 551 (2005)].

[30] M. L. Trunov, J. Optoelectr. Adv. Mater. **7**, 1223 (2005).

[31] N. G. Olson, C. Leung, X. Wang, Experimental Techniques **12**, 51 (2002).

[32] W. C. Oliver, G. M. Pharr, J. Mater. Res., **7**, 1564 (1992).

[33] S. Suzuki, M. Takahashi, T. Kobayashi, J. Non-Cryst. Solids **46**, 163 (1981).

[34] Anthony C. Fischer-Cripps, Nanoindentation Springer-Verlag, New-York (2004).

[35] A. Feltz, Amorphous Inorganic Materials and Glasses, VCH, (1993).

[36] K. Schwartz, The Physics of Optical Recording, Springer-Verlag, Berlin (1993).

[37] V. S. Bilanich, A. A. Gorvat, Fizika i Khimia Stekla (Sov. J. Glass. Phys. Chem.) **24**, 825 (1998).

[38] J. Perez, B.Duperray, D.Lefevre, Non-Cryst. Solids **44**, 113 (1981).

[39] A. Kolobov, H. Oyanagi, K. Tanaka, Ke. Tanaka, Phys. Rev. B **55**, 726 (1997).

[40] G. M Bartenev, S. Ya. Frenkely, Physics of polymers (in Russian), "Khimia" Publishing House, Leningrad (1990).

[41] G. M. Bartenev, D. S. Sanditov, Relaxation Processes in Vitreous Systems (in Russian), "Nauka" Publishing House, Novosibirsk (1986).

[42] H. Hisakuni, K. Tanaka, Opt. Lett. **20**, 958 (1995).

[43] G. Marsh, Materials Today **6**, 38 (2003).

[44] H. G. Mamin, B. D. Terris, L. S. Fan, S. Hoes, R. C. Barrett, D. Rugar, IBM J. Res. Develop. **39**, 681(1995).

[45] Y. Lu, D. B. Shao, S. C. Chen, Appl. Phys. Lett. **85,** 1604 (2004).